

Predictive airframe maintenance strategies using model-based prognostics

Proc IMechE Part O:
J Risk and Reliability
1–20
© IMechE 2018
Reprints and permissions:
sagepub.co.uk/journalsPermissions.nav
DOI: 10.1177/1748006X18757084
journals.sagepub.com/home/pio


Yiwei Wang^{1,2}, Christian Gogu², Nicolas Binaud²,
Christian Bes², Raphael T Haftka³ and Nam-Ho Kim³

Abstract

Aircraft panel maintenance is typically based on scheduled inspections during which the panel damage size is compared to a repair threshold value, set to ensure a desirable reliability for the entire fleet. This policy is very conservative since it does not consider that damage size evolution can be very different on different panels, due to material variability and other factors. With the progress of sensor technology, data acquisition and storage techniques, and data processing algorithms, structural health monitoring systems are increasingly being considered by the aviation industry. Aiming at reducing the conservativeness of the current maintenance approaches, and, thus, at reducing the maintenance cost, we employ a model-based prognostics method developed in a previous work to predict the future damage growth of each aircraft panel. This allows deciding whether a given panel should be repaired considering the prediction of the future evolution of its damage, rather than its current health state. Two predictive maintenance strategies based on the developed prognostic model are proposed in this work and applied to fatigue damage propagation in fuselage panels. The parameters of the damage growth model are assumed to be unknown and the information on damage evolution is provided by noisy structural health monitoring measurements. We propose a numerical case study where the maintenance process of an entire fleet of aircraft is simulated, considering the variability of damage model parameters among the panel population as well as the uncertainty of pressure differential during the damage propagation process. The proposed predictive maintenance strategies are compared to other maintenance strategies using a cost model. The results show that the proposed predictive maintenance strategies significantly reduce the unnecessary repair interventions, and, thus, they lead to major cost savings.

Keywords

Structural airframe maintenance, model-based prognostics, predictive maintenance, extended Kalman filter, first-order perturbation method

Date received: 31 May 2017; accepted: 1 January 2018

Introduction

Aircraft maintenance represents a major economic cost for the aviation industry. In 2015, the maintenance, repair, overhaul (MRO) market value was three-quarters of the whole aircraft production market value. Developing efficient maintenance can be an important way for airlines to allow a new profit growth. Aircraft maintenance can be classified into airframe maintenance and engine maintenance. Airframe maintenance that deals with non-structural items is called non-structural airframe maintenance,¹ while the one concerned with fatigue damage in the structural sections, such as fuselage panels, is called structural airframe maintenance. In this article, the maintenance is limited

to structural airframe maintenance for fatigue cracks in fuselage panels.

¹School of Mechanical Engineering, Nanjing University of Science and Technology, Nanjing, China

²Université de Toulouse, Institut Clément Ader (ICA), CNRS, INSA/UPS/ISAE/Mines Albi, Toulouse, France

³Department of Mechanical & Aerospace Engineering, University of Florida, Gainesville, FL, USA

Corresponding author:

Christian Gogu, Université de Toulouse, Institut Clément Ader (ICA), CNRS, INSA/UPS/ISAE/Mines Albi, 3 Caroline Street Aigle F-31400 Toulouse, France.
Email: christian.gogu@gmail.com

Traditional aircraft maintenance is highly regulated based on a fixed maintenance schedule (thus called scheduled maintenance) to ensure safety and correct functionality between maintenance intervals. For example, under the Federal Aviation Administration (FAA), operators are required to prepare a mandatory Continuous Airworthiness Maintenance Program (CAMP). CAMP includes both routine and detailed inspections, which are generally referred to as “checks” by airlines. There are four levels of checks, termed A, B, C, and D, from lighter to most thorough. A and B checks are lighter checks, taking from dozens of man-hours to hundreds of man-hours. C and D checks are thorough checks, during which the aircraft is partially disassembled to undergo a series of maintenance activities including both engine and airframe maintenance. The inspections are often implemented by techniques such as non-destructive inspection (NDI), general visual inspection (GVI), detail visual inspection (DVI), which lead to significant downtime of up to 1 month.

With progress in sensor technology, structural health monitoring (SHM) systems, which employ a sensor network embedded inside aircraft structures to monitor damage, are gradually being introduced in the aviation industry.^{2–5} Once it is possible to monitor the structural damage state automatically and continuously, more advanced condition-based maintenance (CBM) can be implemented.⁶ CBM is defined by the maintenance being triggered by an event when some conditions are satisfied. For structural airframe maintenance, CBM is based on the actual condition of the aircraft, rather than fixed inspection routines that might not be necessary, and thereby reduces aircraft downtime and reduces maintenance cost.

Much attention has been paid to CBM strategies in the literature^{7–9} and more recently to predictive maintenance (PdM).^{10–15} CBM and PdM share some characteristics in common that both rely on damage assessment data collected by the SHM system. The difference lies in that CBM makes decisions based on the current damage level, while PdM makes use of, in addition to current damage information, a prognostics index to make the decision. The remaining useful life (RUL) is the most common prognostics index.¹⁶ The RUL-based PdM decides the next maintenance based on the estimated RUL.^{14,17,18} For aircraft maintenance, however, the standards are set by the International Civil Aviation Organization (ICAO) and implemented by national and regional bodies around the world. Arbitrarily deciding on structural airframe maintenance time only based on the estimated RUL without considering the scheduled maintenance (during which the engine and non-structural airframe maintenance are also performed) can be disruptive to the current maintenance practice. In addition, RUL-triggered maintenance is not optimal from an economic point of view due to less notification in advance, for example, the absence of maintenance crews or lack of a spare part. Therefore, for structural airframe maintenance, it

would be more desirable to predict the probability that an airframe structure would operate normally up to given future time.¹⁹ In other words, use the predicted reliability as the prognostics index. The PdM policy that incorporates the predicted reliability information for supporting decision-making can be found in the literature.^{10,13,15}

For the application of structural airframe maintenance for a fleet of aircraft, Pattabhiraman et al.¹ proposed two CBM strategies, aiming at reducing the number of traditional scheduled maintenance. One strategy is purely CBM, that is, triggering maintenance anytime when needed, based only on the current panel damage state. The other strategy takes into account the scheduled maintenance stops. In their approaches, an SHM system is used to monitor the damage state of the aircraft as frequently as needed. Using the measured crack sizes, the maintenance decisions are developed based on some fixed thresholds. These thresholds are determined for the entire fleet of aircraft to ensure a desirable level of reliability. There are two shortcomings in the work of Pattabhiraman et al. First, they assume that the SHM data are perfect, which may be impractical since due to the sensor limitations and harsh working conditions, the data always contain noise and disturbances. Second, Pattabhiraman et al. used two different thresholds, corrective threshold and preventive threshold, to distinguish a corrective repair and a preventive repair (the preventive threshold is much smaller than the corrective one). Corrective repair is carried out when the damage level of the panels exceeds a corrective threshold. Preventive repair is carried out at the time of corrective repair to repair the panels whose damage level exceeds the preventive threshold but is lower than the corrective threshold. The objective of predictive repair is economic, for example, to reduce the number of maintenance stops. Although Pattabhiraman considered two types of repair, the corrective threshold and the preventive threshold are fixed for all the panels in the fleet. This could be suboptimal since damage growth rate may vary from panel to panel. Therefore, a conservative threshold has to be adopted to ensure the safety of the whole fleet.

This article thus aims to go further in terms of optimizing the maintenance process, by moving from CBM to PdM with the potential for further cost savings. We therefore adopt the second type of prognostics index, that is, the *predicted reliability*, for reducing the conservativeness caused by the use of fixed thresholds for the entire fleet. To this end, we use a model-based prognostics method, called EKF-FOP method that couples the extended Kalman filter (EKF) and first-order perturbation (FOP), developed in our previous work.²⁰ EKF-FOP allows to make the repair decision taking into account the future reliability of each individual panel rather than a fixed threshold for all panels. The EKF-FOP method has two functions: filtering measurement noise to give a better estimate of damage level (achieved

by EKF) and predicting the damage distribution in the future (achieved by FOP). Once the damage distribution of a panel is predicted, the reliability of the panel at a given future time is calculated. This *predicted reliability information* is used to form the repair policy, which is the core of the PdM presented in this article. Similar to Pattabhiraman, we propose two strategies: PdM considering the aircraft scheduled maintenance stops and predictive maintenance-skip (PdM-skip) the other way around. The performance of PdM and PdM-skip is assessed through a cost model by comparing with Pattabhiraman's two CBM strategies and the traditional scheduled maintenance.

The remainder of this article is organized as follows. Section "Model-based prognostics for individual fuselage panel" briefly recalls the model-based prognostics method proposed in the literature²⁰ for the application of fatigue crack prognosis. Section "PdM strategies using model-based prognostics" details the developed PdM strategies when the model-based prognostics method is used. Section "Numerical examples" implements numerical experiments on a fleet of short-range commercial aircraft. Benefits of the PdM using model-based prognostics are shown in terms of scheduled and unscheduled repair as well as in terms of maintenance cost reduction. Finally, in section "Conclusion," we draw conclusions and suggest potential future research work.

Model-based prognostics for individual fuselage panel

Prognostic methods can generally be grouped into data-driven and model-based methods. For the application of fatigue crack prognosis, a model-based method is adopted here since fatigue damage models for metals have been well studied.^{21,22} Model-based prognostics methods involve three issues. (1) A physical model with unknown model parameters describing the degradation process is assumed to be available. (2) The damage state and the model parameters need to be estimated from the measurement data collected up to the current time. (3) The distribution of future damage state needs to be predicted based on the estimated damage state and estimated model parameters.

For the first issue, the well-known Paris model is used for fatigue crack propagation, as given in equation (1), in which a is the half-crack size in meters, k is the number of load cycles, da/dk is the crack growth rate in meter/cycle, and m and C are the Paris model parameters. Throughout this article, we use the terms "Paris model parameters," "model parameters," and "material parameters" interchangeably to refer to m and C . ΔK is the range of stress intensity factor, which is given in equation (2) as a function of the pressure differential p , fuselage radius r , and panel thickness t . The coefficient A in the expression for ΔK is a correction factor intended to compensate for modeling the fuselage as a hollow cylinder without stringers and stiffeners.¹ The

two parameters m and C are assumed unknown that need to be estimated from the measurement data

$$\frac{da}{dk} = C(\Delta K)^m \quad (1)$$

$$\Delta K = A \frac{pr}{t} \sqrt{\pi a} \quad (2)$$

The crack growth can be modeled in myriad ways depending on whether the critical site is subjected to multiple-site damage, widespread fatigue damage, two-bay crack or other types of fatigue damage. A study conducted by Molent and Barter²³ reviewed fatigue crack growth data from a significant number of full-scale fatigue test (FSFT) on several different military aircraft types. In the FSFT, the airframe was subjected to loads of varying amplitude and complexity for a specified period of testing. They concluded that a simple crack growth model adequately represents a typical crack growth. Here the well-known Paris model is employed since it is widely used for modeling fatigue crack growth.^{24,25}

For the second issue, several techniques can be considered, for example, EKF, particle filter (PF), and nonlinear least squares (NLS). EKF and PF are based on recursive Bayesian inference, which estimates the state and parameters recursively by taking one datum at a time.²⁶ Therefore, they are able to deal with the real-time estimation of state and parameters as the data arrive sequentially. In contrast, NLS processes all data simultaneously in a batch, indicating that the computational complexity increases as time evolves and as more data are available. In this article, the crack propagation process is modeled as a hidden Markov model (HMM, or general state-space model²⁷) since we assume that the evolution of crack size is hidden but can be observed through measurement data that contain noise. HMM is widely used to model degradation processes.^{28,29} In this context, filtering methods are most appropriate. Here EKF is chosen due to its computational efficiency and robustness. EKF gives estimates of crack size and model parameters as well as their uncertainty (represented by the covariance matrix). Note that identifying the uncertainty structure (covariance matrix) is necessary in order to be able to estimate the future reliability index.

For the third issue, once the state and parameters are estimated, the future behavior of degradation can be easily predicted. A straightforward way is Monte Carlo (MC) simulation, that is, generating samples based on the estimated joint distribution of state-parameters given by EKF and propagating these samples through the Paris model for a given future time. The idea of using MC simulation is illustrated in Figure 1. Alternatively, we propose a linearization method called FOP method to calculate the evolution of crack size distribution analytically. One advantage of the FOP method over the MC simulation is reduced computational cost. This advantage might not matter when dealing with one individual crack growth process in one fuselage panel, but it is significant when applied to a fleet of aircraft comprising hundreds or thousands of aircraft panels.

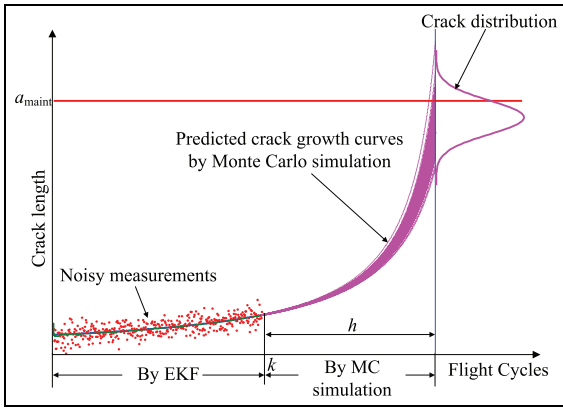


Figure 1. Using Monte Carlo method to predict future degradation.

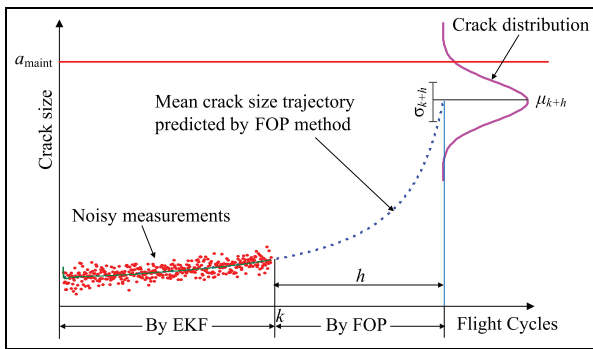


Figure 2. Schematic diagram of EKF-FOP method.

The process of how to model the crack propagation as a Hidden Markov Model as well as the details of the developed EKF-FOP method were presented in sections 2, titled ‘state-space method for modeling the degradation process’, and section 3, titled ‘prognostics method for individual panel’ in Wang et al.²⁰ For the sake of completeness, the method is summarized in Appendix 1. Only the necessary notations for the following narrative are presented here. The crack size and two Paris model parameters estimated by EKF at cycle k are denoted as \hat{a}_k , \hat{m}_k , and \hat{C}_k , respectively. The predicted mean and standard deviation of the crack size given by FOP method after h cycles beyond the current cycle k are denoted as μ_{k+h} and σ_{k+h} , respectively. The schematic diagram of EKF-FOP method is illustrated in Figure 2.

To verify the accuracy of the proposed FOP method for future degradation prediction, we compare the predicted crack size distribution given by FOP method and the one given by MC simulation for a length of time beyond the last measurement. The comparison is detailed in Appendix 2. We find that the predicted mean and standard deviation with the FOP method are within a few percent of those predicted by the MC method; however, the FOP method is about 4800 times computationally cheaper than MC. Moreover, we evaluate the performance of the EKF-FOP method by comparing with true known RUL using five established prognostics metrics:³⁰ prognostics horizon (PH), $\alpha - \lambda$

accuracy, relative accuracy (RA), cumulative relative accuracy (CRA), and convergence. The results are reported in Appendix 3. The results show that the proposed prognostics method performs well according to all five prognostic metrics.

PdM strategies using model-based prognostics

In this section, two variants of PdM strategies are developed using the model-based prognostics method introduced in the previous section. Recall that our objective is to plan the structural airframe maintenance considering that the engine and non-structural airframe maintenance are always performed at the time of scheduled maintenance.

Maintenance assumptions

The employment of SHM system allows the possibility of planning maintenance based on the actual health state of the aircraft rather than on a fixed schedule. However, as mentioned before, arbitrarily triggering maintenance might be a bit disruptive to the traditional scheduled maintenance, during which the engine and non-structural airframe maintenance are carried out. On the other hand, it makes sense to skip some scheduled maintenance at the early stage of the aircraft lifecycle since the frequency of scheduled maintenance for commercial aircraft is designed very conservatively. It is highly likely that no panels need to be repaired at the earlier stage of the aircraft lifecycle.

For the scheduled maintenance, the aircraft undergoes the routine maintenance according to the schedule $T_b = T_1 + (b-1)\Delta T$, where b is the counter of maintenance stops, T_1 the flight cycle of the first scheduled maintenance stop, and ΔT the interval between two consecutive scheduled maintenance stops. The scheduled maintenance time $\{T_b\}$ is defined by aircraft manufacturers in concert with certification authorities. Therefore, it is assumed to be fixed.

The SHM system is assumed to monitor the damage state of each panel in the fuselage. The frequency of damage status evaluation, henceforth called damage assessment, is assumed every 100 flights, which coincides with the A-check. It would make sense to carry out the SHM-based maintenance at a frequency of 100 cycles if the sensors themselves are embedded in the aircraft and the monitoring system is ground-based to reduce flying weight and monitoring system cost.¹

Although our application objective is a fuselage that contains hundreds of panels, panels are treated independently and their structural dependency is not considered. That makes sense because unlike the system having a k -out-of- n : F structures (i.e. the system fails if at least k of the n components fail) or the $(n-k+1)$ -out-of- n : G structures (the system works if at least $(n-k+1)$ of the n components work), the malfunction

of one panel does not affect that of other panels. One can refer to the literature^{10,14} for maintenance policy considering structural dependency.

The critical half-crack size that will cause panel failure can be calculated by equation (3). Based on linear elastic fracture mechanics, equating the stress intensity factor in mode I (cf. equation (2)) to the fracture toughness K_{IC} leads to the critical crack size a_{cr} as shown in equation (3), where p_{cr} is a conservative estimate of the pressure differential. Since the damage assessment is done every 100 cycles and no intervention is performed between 100 cycles, an additional safety threshold, denoted as a_{maint} , is introduced to maintain a desirable reliability between 100 cycles. a_{maint} is calculated to maintain a $1E-7$ probability of failure of the aircraft between two damage assessments, that is, when a crack size exceeding a_{maint} is present on the aircraft, its probability to exceed the critical crack size a_{cr} in the future 100 cycles is less than $1E-7$. A $1E-7$ probability of failure is a typical reliability used in aircraft damage tolerance design.^{1,31} By repairing panels having cracks larger than a_{maint} , one ensures the safety of the aircraft until the next damage assessment

$$a_{cr} = \left(\frac{K_{IC}}{A \frac{p_{cr}}{t} \sqrt{\pi}} \right)^2 \quad (3)$$

Repair policy for individual crack propagation process

The EKF-FOP method introduced in the previous section is used to develop the repair policy. According to EKF-FOP method, when measurement data are available up to the k th cycle, the EKF is used to estimate the crack size and the Paris model parameters at the k th cycle. Based on the estimated crack size and material parameters, that is, \hat{a}_k , \hat{m}_k , and \hat{C}_k , the FOP method is used to predict the evolution of the crack size in the next h cycles. As per EKF-FOP, the distribution of the crack size is a normal distribution. The mean and standard deviation of the crack size at $k + h$, μ_{k+h} and σ_{k+h} , are calculated by the FOP method. Based on the predicted crack size distribution, we calculate the 0.95 quantiles, denoted by a_q

$$a_q(h) = \Phi^{-1}(0.95 | \mu_{k+h}, \sigma_{k+h}) \quad (4)$$

in which Φ^{-1} is the inverse cumulative distribution function of the normal distribution with mean and standard deviation μ_{k+h} and σ_{k+h} , respectively. If $a_q > a_{maint}$, the panel is considered in danger and should be repaired. Otherwise, this panel is left unattended. This repair decision is denoted by d , which has a binary value

$$d = \begin{cases} 0 & \text{if } a_q \leq a_{maint} \\ 1 & \text{if } a_q > a_{maint} \end{cases} \quad (5)$$

The underlying meaning behind the repair policy is that if a panel has a crack with the size \hat{a}_k , the

probability that this crack grows greater than the threshold a_{maint} at the next scheduled maintenance is less than 5%. Note that the level of the quantile (95% here) controls the conservativeness of the estimation and can be seen as a tuning parameter of the strategy. This conservativeness level is not, however, intended to guarantee the safety of the aircraft. The safety of the aircraft will be guaranteed by an additional branch of the maintenance strategy, which will be described later. Through an empirical study, we found that the cost of the proposed maintenance strategies is relatively insensitive to the value of the quantile, so in the rest of the paper it is fixed to 95%. Note also that the forward prediction interval h varies depending on different strategies and can be seen as another tuning parameter of the strategy. This tuning parameter was found to have more impact on cost, and its tuning will be addressed in the subsequent sections.

PdM

The objective of PdM is to decide on maintenance according to the actual condition of an aircraft rather than based on a fixed maintenance schedule. Figure 3 illustrates the flowchart of PdM. In this strategy, damage assessment is implemented every 100 cycles. At each damage assessment, the EKF is used to calculate the estimated crack size of all the panels in an aircraft. If the largest crack size exceeds a_{maint} , an unscheduled maintenance is asked immediately and the aircraft is sent to the maintenance hangar. The panel with the largest crack size triggering the unscheduled maintenance is called the critical panel. At an unscheduled maintenance stop, besides repairing the critical panel, other panels may be also repaired according to the repair policy presented in the previous subsection to prevent frequent unscheduled maintenance. More specifically, for the i th panel, its crack size distribution in the next $h = I_{PdM}$ cycles is predicted and the 0.95 quantile of the predicted crack size, denoted as $a_q^i(I_{PdM})$, is calculated. The panels whose $a_q^i(I_{PdM})$ is greater than a_{maint} are repaired. The value of forward prediction interval I_{PdM} can be optimized. Following an empirical study with different I_{PdM} values, we set $I_{PdM} = 23,000$ cycles which was found to lead to the lowest maintenance costs.

PdM-skip

Despite the advantage of PdM, it also has some drawbacks. The PdM applies only to structural airframe maintenance. The engine and non-structural airframe maintenance are always implemented at scheduled maintenance. PdM that triggers unscheduled maintenance may disturb the original scheduled maintenance. In addition, having the structural airframe maintenance at the same time with the engine and non-structural maintenance would tend to reduce cost. Therefore, it would be beneficial that the traditional scheduled

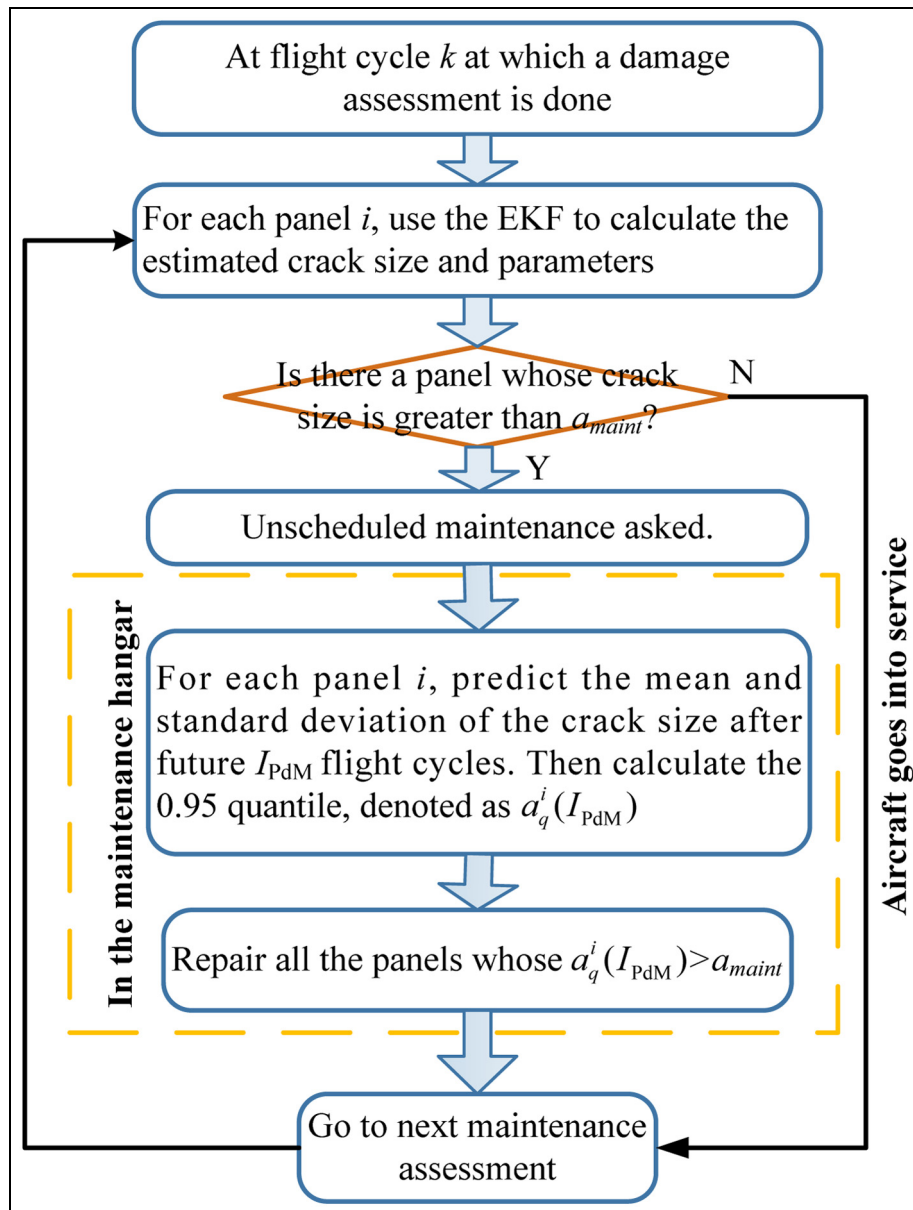


Figure 3. Flowchart of PdM strategy for an aircraft.

maintenance works in tandem with the unscheduled maintenance. PdM-skip is developed to meet this goal that leverages the strength of both scheduled maintenance and PdM.

The PdM-skip process is described in Figure 4. The damage assessment is carried out at scheduled maintenance time as well as every 100 cycles. At each scheduled maintenance stop, for an aircraft, there are two decision levels. The first level is a maintenance decision that decides to skip or to trigger the current scheduled maintenance for the aircraft. The second level decision is a repair decision regarding which panels should be repaired once the current scheduled maintenance is triggered.

Specifically, the maintenance decision is implemented as follows. At each scheduled maintenance, before the aircraft goes to the maintenance hangar, for the i th panel, its crack size distribution after next $h = \Delta T$

cycles is predicted (i.e. the distribution at the next scheduled maintenance) and the 0.95 quantile of the predicted crack size distribution, denoted as $a_q^i(\Delta T)$, is calculated. If there is no panel whose $a_q^i(\Delta T)$ exceeds a_{maint} , the current scheduled maintenance is skipped. Otherwise, the current scheduled maintenance is triggered and the aircraft is sent to the maintenance hangar. The objective of setting the forward prediction interval $h = \Delta T$ is to avoid unscheduled maintenance between two consecutive scheduled maintenance stops.

For an aircraft sent to the hangar, the repair decision is implemented as follows for all the panels. For the i th panel, its crack size distribution until the end of life (EOL) of the aircraft is predicted. The forward prediction interval h equals to the aircraft lifetime k_{EOL} minus the current cycle k , i.e., $h = k_{EOL} - k$. The 0.95 quantile of the predicted crack size distribution,

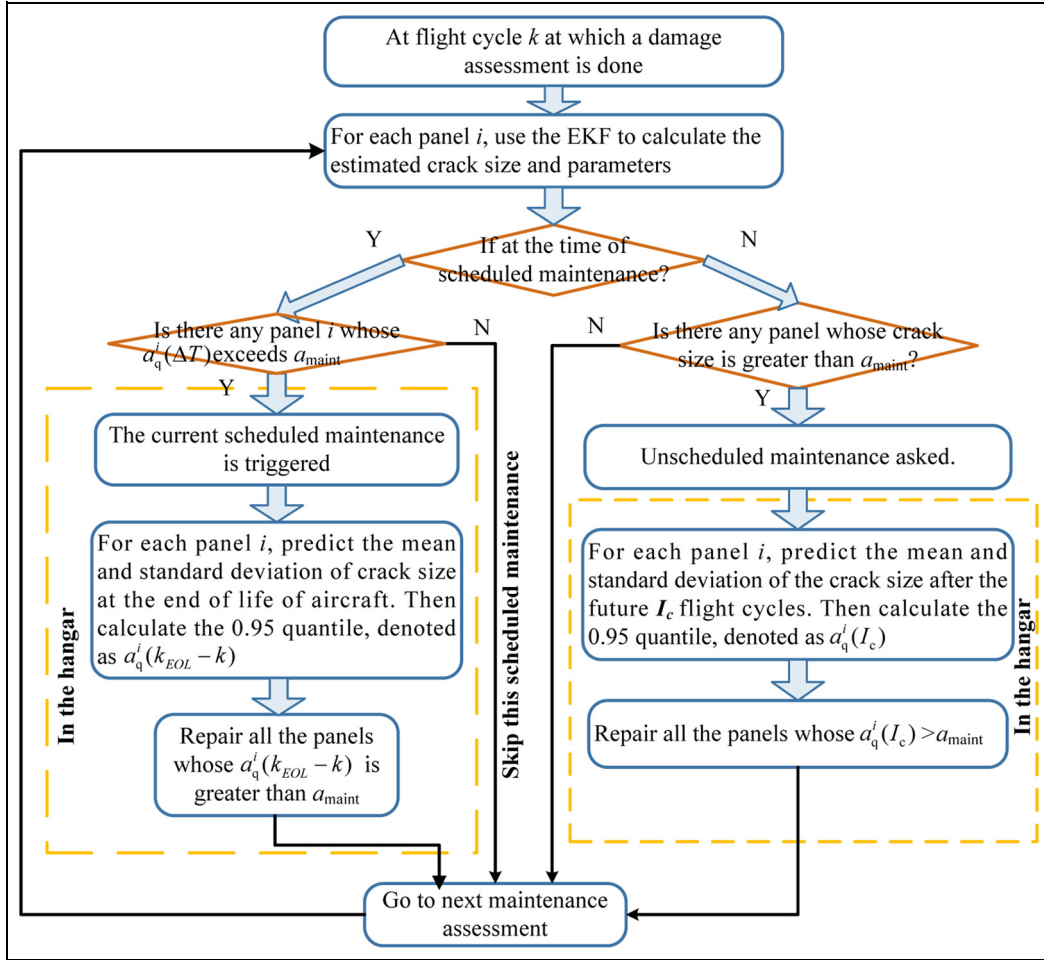


Figure 4. Flowchart of PdM-skip strategy.

denoted as $a_q^i(k_{EOL} - k)$, is calculated. All the panels whose $a_q^i(k_{EOL} - k)$ exceed a_{maint} are repaired.

If a crack that is missed at the time of scheduled maintenance exceeds a_{maint} between two consecutive scheduled maintenance stops, PdM-skip will recommend maintenance to be performed immediately. This calls for unscheduled maintenance, which is costlier but guarantees safety. At an unscheduled maintenance stop, we predict the crack size distribution in the future I_c cycles for all panels and then decide on the ones that need to be repaired according to the repair policy. I_c is set to be the number of cycles from current to the scheduled maintenance after the next one. This is intended to be able to skip the next scheduled maintenance and not have an unscheduled maintenance soon after. For example, if the scheduled maintenance is every 4000 cycle and an unscheduled maintenance occurs at the 43,000th cycle, I_c will be set to 5000 in order to have the next maintenance at 48,000 cycles by skipping the one at 44,000 cycles.

Cost model

The aircraft maintenance cost is composed of engine maintenance cost and airframe maintenance cost. The airframe maintenance cost is further divided into

structural airframe and non-structural airframe maintenance. In this article, we focus on structural airframe maintenance cost. Note that the engine and non-structural maintenance are always performed at the time of scheduled maintenance interval. The cost of the structural airframe maintenance performed by traditional NDI or DVI technologies at the time of a scheduled maintenance stop consists of two parts, the setup cost c_0 and the repair cost. The repair cost equals the cost of repairing one panel, denoted by c_s , multiplied by the number of repaired panels. c_0 is assumed US\$1.44 and c_s is US\$ 0.25 million as per Kundu.³²

In the PdM and PdM-skip, the damage inspection is performed by the on-board SHM system; hence, at the scheduled maintenance, the setup cost will be only a fraction of the cost of the traditional scheduled maintenance. This fraction is denoted as K_{SHM} and is set to be 0.7.¹ The setup cost at an unscheduled structural airframe maintenance trip is higher due to less advance notice, as well as the fact that the structural airframe maintenance and the other maintenance (engine, non-structural) are not done at the same time. A factor K_{un} is set to denote the higher setup cost incurred for unscheduled maintenance and $K_{un} = 2$ is taken.¹ The cost of structural airframe maintenance is thus given as

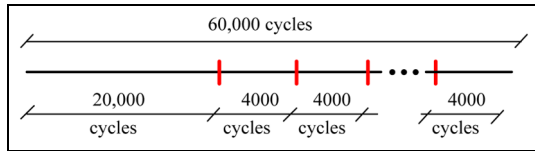


Figure 5. Scheduled maintenance, cycles represent the number of flights.

$$C_{\text{main}} = N_s K_{\text{SHM}} c_0 + N_{\text{us}} K_{\text{un}} c_0 + c_s N_{\text{rp}} \quad (6)$$

where N_s is the number of triggered scheduled maintenance stops, N_{us} is the number of unscheduled structural maintenance trips, and N_{rp} is the number of repaired panels during the whole lifetime of an aircraft.

Numerical examples

Our application objective is a typical short-range commercial aircraft with a typical lifetime of 60,000 flight cycles. We consider a fleet of 100 such airplanes with 500 fuselage panels per aircraft. Each panel is assumed to have one initial crack, with initial crack size following a lognormal distribution. Traditionally for this type of aircraft, the first maintenance is performed after 20,000 flight cycles and subsequent maintenance is every 4,000 cycles until the EOL, for a total of 10 scheduled maintenance stops in 60,000 cycles, as shown in Figure 5.

We evaluate the performance of PdM/PdM-skip by comparing with two other strategies. The first strategy is the traditional scheduled maintenance, whose schedule is shown in Figure 5. At each scheduled stop, the aircraft is taken into a hangar and the inspection of all panels is done using techniques like NDI or DVI. Cracks detected with a size greater than a threshold are repaired. The threshold is determined to guarantee a desirable level of probability of failure between two scheduled maintenance stops and is fixed for all panels in the fleet. Therefore, this strategy is threshold based.

The second strategy has two variants due to Pattabhiraman et al.,¹ CBM and CBM-skip, in which the damage assessment is done every 100 flights using SHM. Details about CBM and CBM-skip are given in Appendix 4. In CBM, at each damage assessment, if the largest crack size in an aircraft exceeds a_{maint} , unscheduled maintenance is triggered immediately and all the panels with a crack size larger than a repair threshold $a_{\text{rep-CBM}}$ are repaired.

In contrast, CBM-skip takes into account the scheduled maintenance but aims at skipping some unnecessary early scheduled maintenance stops. Specifically, at each scheduled maintenance stop, if there is no crack size exceeding a threshold $a_{\text{th-skip}}$, then the current scheduled maintenance is skipped. Otherwise, the current scheduled maintenance is triggered and the panels with crack size greater than a repair threshold $a_{\text{rep-skip}}$ are repaired. If there is a crack that grows beyond a_{maint} between two consecutive scheduled maintenance

stops, then an unscheduled maintenance stop is triggered at once, and all panels with crack size greater than $a_{\text{rep-skip}}$ are repaired.

CBM and CBM-skip are also threshold-based since the thresholds are the same for the entire fleet. Since our work is an extension on the top of the work of Pattabhiraman's, we seek to compare the threshold-based maintenance proposed by Pattabhiraman and our prognostics-based maintenance. Note that in CBM and CBM-skip, the reliability is controlled by the safety threshold a_{maint} , while $a_{\text{rep-CBM}}$, $a_{\text{rep-skip}}$, and $a_{\text{th-skip}}$ are tuning parameters affecting the cost that can be optimized. The same value of a_{maint} is used in CBM, CBM-skip, PdM, and PdM-skip, that is to say, all strategies are compared under the same safety level.

Besides the strategies themselves, another significant difference between Pattabhiraman's work and our work is the treatment of the pressure p . Pattabhiraman treated it as a constant while we have taken into account its uncertainty during the crack propagation and modeled it as a normal random variable. In order to maintain consistency and to make our work comparable, we introduce the uncertainty of p into Pattabhiraman's strategies. Accordingly, the thresholds used in CBM/CBM-skip are modified to adapt to the introduction of uncertainty on p .

Input data

The values of the geometry parameters defining the fuselage (i.e. fuselage radius, panel thickness) used here are typical of short-range commercial aircraft. These values are time-invariant. Recall that we define a correction factor A for stress intensity factor, which accounts for the fact that the fuselage is modeled as a hollow cylinder without stringers and stiffeners. The numerical values for the geometry parameters have been chosen from the literature¹ and are reported in Table 1.

The values of thresholds are determined as follows. The critical crack size a_{cr} is calculated by equation (3) as $a_{\text{cr}} = 59.6$ mm. The safety threshold a_{maint} is calculated to maintain a $1\text{E-}7$ probability of panel failure between two damage assessments (every 100 cycles) and $a_{\text{maint}} = 47.4$ mm. To make CBM and CBM-skip as cost-efficient as possible, it is necessary to find the optimal value of $a_{\text{rep-CBM}}$, and the optimal combination of $a_{\text{rep-skip}}$ and $a_{\text{th-skip}}$. For this purpose, we carried out an empirical trade-off study by considering a grid within the range [2, 15] mm for $a_{\text{rep-CBM}}$, [2, 12] mm for $a_{\text{rep-skip}}$, and [2, 15] mm for $a_{\text{th-skip}}$, all with an increment of 0.1 mm. Based on the evaluations of these grid points, we found that the values $a_{\text{rep-CBM}} = 4.8$ mm, $a_{\text{rep-skip}} = 4.0$ mm, and $a_{\text{th-skip}} = 7.0$ mm lead to the lowest maintenance cost according to the cost model in equation (6).

For simulating the maintenance process of a fleet, we consider two types of uncertainties that are different in nature, that is, aleatory and epistemic uncertainty.³³ Aleatory uncertainty represents the intrinsic variability

among populations that cannot be reduced by further data. In our context, it can be interpreted as follows. Even if the panels are made of the same materials, the material parameters of different panels may not be the same. In addition, due to the intrinsic variability in crack initiation, each panel has different initial crack sizes. In this study, the aleatory uncertainty is modeled by assuming that the initial crack size a_0 and the material parameters follow some prescribed distributions. Specifically, the initial crack size a_0 is assumed lognormally distributed while m and $\log_{10}C$ are assumed to follow a multivariate normal distribution with a negative correlation coefficient, based on the literature.^{22,34,35} The prescribed distributions are reported in Table 2. Before starting the simulation, 100×500 samples of initial crack size and the model parameters are randomly drawn from their respective distributions and assigned to each panel. Specifically, the initial crack size is generated from the lognormal distribution while the two model parameters are generated from the multivariate normal distribution and denoted as $a_0(i)$, $m(i)$ and $\log_{10}C(i)$ ($i = 1, 2, \dots, 50,000$), respectively. $m(i)$ and $\log_{10}C(i)$ are regarded as the “true but unknown” material parameters of an individual panel (here “unknown” means the material parameters contain epistemic uncertainty, which will be discussed next). The 50,000 generated samples of the materials parameters are illustrated in Figure 6.

The aleatory uncertainty relates to the variability in the population of the panels. Now we discuss the crack growth process in each individual panel. For an individual panel, its material parameters, $m(i)$ and $\log_{10}C(i)$, are not random in nature but deterministic. However, due to lack of knowledge, they are unknown or poorly known. This kind of uncertainty is epistemic uncertainty and can be reduced by collecting more relevant data. In our case, the material parameters are estimated from noisy measurements by the EKF algorithm, and furthermore, the estimation uncertainty reduces as time evolves due to more data being available.

The measurement data used in this article are simulated as follows: (1) using $a_0(i)$, $m(i)$, and $\log_{10}C(i)$ ($i = 1, 2, \dots, 50,000$) to compute the true crack size based on the Paris model and (2) adding the following measurement noise to the true crack size: Gaussian noise with mean zero and standard deviation $\sigma = 0.03E-3$ (10% coefficient of variation with respect to the mean of initial true crack size in Table 2, that is, $0.3E-3$). The measurements are collected every 100 cycles, being consistent with the interval of damage assessment. At each time of damage assessment, the EKF is applied to estimate the crack size and the Paris model parameters. We choose Gaussian noise based on its wide use to simulate a realistic noisy signal. It is a good assumption for the process or system that is subject to the central limit theorem.³⁶ In the absence of information indicating otherwise, Gaussian noise is thus used to model measurement noise under the

Table 1. Aircraft geometry parameters.

Description	Notation	Value
Fuselage radius	r	1.95 m
Panel thickness	t	$2e-3$ m
Correction factor	A	1.25

Table 2. Uncertainties on a_0 , $[m, C]$.

Description	Notation	Type	Value
Initial crack size (m)	a_0	Lognormal	$\text{LnN}(0.3e-3, 0.08e-3)$
Paris model parameters	$[m, C]$	Multivariate normal	$N(\mu_m, \sigma_m, \mu_C, \sigma_C, \rho)$
Mean of m	μ_m	—	3.6
Mean of C	μ_C	—	$\log_{10}(2e-10)$
CC of m and C	ρ	—	-0.8
SD of m	σ_m	—	3% COV
SD of C	σ_C	—	3% COV

CC: correlation coefficient; SD: standard deviation; COV: coefficient of variation.

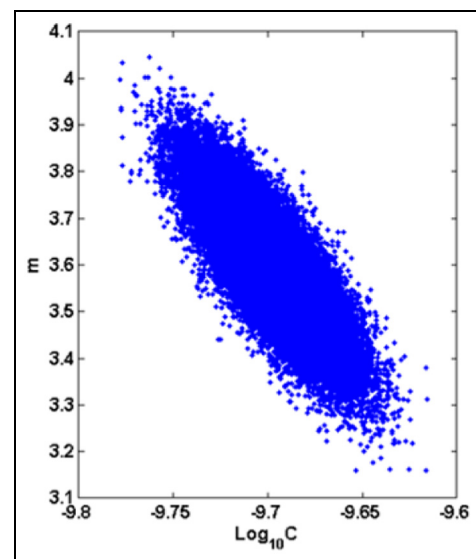


Figure 6. Illustration of the population of $\{m, C\}$.

assumption of numerous sources of uncertainty and the central limit theorem.

It is difficult to get actual data for aircraft fuselage panels since the widespread deployment of SHM systems in commercial aircraft is still at the research stage. Tests have been done during the last decades by airlines as well as research centers. The major aircraft operators, regulators, and technology suppliers have been striving for years to standardize SHM integration and certification requirements to mature system for widespread use. Therefore, at this stage, it is difficult to get real data to be used directly in our

Table 3. Comparison of different strategies.

	No maintenance	Scheduled	CBM	CBM-skip	PdM	PdM-skip
Panels failed/repaired over the entire fleet	692 Failures	1403 Repaired	1312 Repaired	1238 Repaired	789 Repaired	798 Repaired
Unnecessary repairs	–	711	620	546	87	106
Minimal no. of maintenance stop	–	10	1	1	1	1
Maximal no. of maintenance stop	–	10	3	4	2	2
Avg. no. of maintenance stop	–	10	1.9	2.2 (0.06)	1.0	1.0 (0)
Minimal no. of repaired panels	–	5	2	3	2	2
Maximal no. of repaired panels	–	21	26	26	16	16
Avg. no. of repaired panels	–	14.03	13.12	12.38	7.89	7.98
Avg. cost of structural maintenance (MUS\$)	–	17.9	8.92	5.50	4.88	3.05

CBM: condition-based maintenance.

approach. Nevertheless, our work is built on realistic assumptions based on existing studies on fatigue crack propagation and can be used readily when measurements are available.

To summarize, we consider a fleet of 100 airplanes with each airplane having 500 fuselage panels. The lifetime of each aircraft is assumed to be 60,000 cycles. Each panel is assumed to have one crack. EKF-FOP method is employed for each individual crack growth process in each panel. The developed two PdM strategies, PdM and PdM-skip, as well as the scheduled maintenance, CBM and CBM-skip are applied to the fleet until the end of the life of the aircraft. The average number of repaired panels, the average number of maintenance stops, and the average structural airframe maintenance cost of the fleet under each strategy are obtained and compared.

Results and discussion

We simulate six processes, that is, no maintenance intervention, scheduled maintenance, CBM, CBM-skip, PdM, and PdM-skip. It should be noted that in the “no maintenance intervention” process, the failure of a panel is defined such that the crack size in that panel exceeds a_{cr} within the lifetime of the aircraft. The comparison results are given in Table 3, in which the second row gives the number of total failures (for the case of no maintenance intervention) or the number of repaired panels (for the five maintenance strategies) over the entire fleet. The third row presents the number of “unnecessarily repaired” panels, that is, panels that would not fail during the whole life but are nevertheless (unnecessarily) repaired according to the maintenance strategy. The fourth to sixth rows give the minimal, the maximal, and the average number of maintenance stops among the 100 aircraft, respectively. The number in the parentheses in the sixth row is the average number of unscheduled maintenance stops in CBM-skip and PdM-skip. Note that for CBM and PdM, all maintenance stops are unscheduled. The seventh to ninth rows give the minimal, the maximal, and the average

number of repaired panels among the 100 aircraft. The last row gives the average cost of structural airframe maintenance over the 100 aircraft in each strategy.

It can be seen that if one lets cracks grow continuously without maintenance intervention, 692 panels over the whole fleet eventually fail. All of these 692 panels are repaired in each maintenance strategy prior to their failure. In other words, all maintenance strategies can ensure safety. Each maintenance strategy has a different extent of “unnecessary repair.” The number of unscheduled maintenance stops is zero in PdM-skip, which indicates that all maintenance occurs at the times of scheduled maintenance stops and no unscheduled maintenance is requested. This does not mean that there will never be any, but it is a rare event that we do not capture with our fleet size.

The results of threshold-based maintenance strategies (i.e. scheduled maintenance, CBM, and CBM-skip) show that CBM and CBM-skip reduce the number of maintenance stops as well as the number of repaired panels compared to the traditional scheduled maintenance, thus reducing the cost significantly. CBM has fewer maintenance stops than CBM-skip (1.9 vs 2.2). However, since CBM is designed independently without taking into account the scheduled maintenance (Figure 5), all CBM stops are unscheduled maintenance and are more costly. In contrast, most of the maintenance stops of CBM-skip occur at the scheduled maintenance. Only very few unscheduled maintenance (0.06 on average) are required. In addition, CBM repairs slightly more panels than CBM-skip because CBM has a larger repair threshold ($a_{rep-CBM} = 4.8\text{ mm}$ vs $a_{rep-skip} = 4\text{ mm}$). Therefore, CBM results in a higher maintenance cost than that of CBM-skip.

In order to analyze the gains of using prognostics-based maintenance strategies (PdM and PdM-skip), we first discuss the *conservativeness*. There are two different contributions to the conservativeness, the inter-aircraft variability and intra-aircraft variability. The former is related to the case when the worst aircraft in the fleet may have a large crack size much sooner than the average, while the latter is related to the case when

different panels in one aircraft have different crack sizes and crack growth rates. The number of unnecessary repairs allows comparing the conservativeness level of the various strategies.

Scheduled maintenance is clearly the most conservative since it needs to cover a very conservative crack size and crack growth rate both over the fleet and within an individual aircraft. In order to decrease the cost, it makes sense to decrease the conservativeness level and the various maintenance strategies reduce the conservativeness to a different extent.

CBM and CBM-skip can address the inter-aircraft variability as well as the intra-aircraft variability related to different crack sizes, but they do not cover intra-aircraft variability related to different crack growth rates. Note that to quantify the conservativeness gains from CBM over the scheduled maintenance, we need to have a comparable number of maintenance stops; otherwise, a higher number of maintenance stops would be traded off for a lower number of repaired panels. Accordingly, we set two stops for scheduled maintenance (closer to the number of stops in CBM 1.9) with a 20,000 cycles interval, that is, the first maintenance stop is at 20,000th and the second is at 40,000th cycle. In this case, the repair threshold decreases to a very small value $0.8E-3m$ to maintain a reliability of $1E-7$ in 20,000 cycles for the entire fleet and the number of repaired panels goes up to 8990.

The conservativeness is further reduced by performing prognostics, which is the main point we want to make in this article. We proposed two prognostics-based maintenance strategies (PdM and PdM-skip); both address the two contributions to the overall conservativeness, and thus decrease simultaneously the number of maintenance stops and repaired panels. On one hand, by setting a long “forward prediction interval” h , the average number of maintenance stops of the fleet in both PdM and PdM-skip reduces to nearly one. On the other hand, due to forecasting the crack growth trend, the number of unnecessary repaired panels is also significantly reduced compared to CBM and CBM-skip (reduction by more than an order of magnitude over CBM and CBM-skip). This is because the proposed PdM considers the crack growth rate for each individual panel, which could not be done in condition-based approaches. The reduction of both of these aspects results in a considerable cost saving over CBM and CBM-skip, which shows the value of using prognostics in the maintenance strategy.

Note that here the forward prediction interval is fixed as 23,000 cycles for PdM and fixed as the number of cycles until EOL for PdM-skip (as a reference, in PdM-skip, earliest time an aircraft in the fleet demands maintenance is at the 36,000th cycle). Therefore, the prediction interval for this aircraft is 24,000 given that the lifetime of aircraft is 60,000 flight cycles. On one hand, a long prediction interval tends to repair more panels at one stop, thus decreasing the frequency of asking for maintenance stops. In fact, we see from Table 3 that the

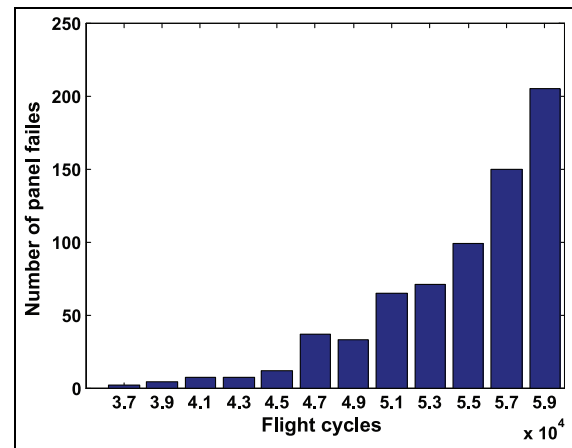


Figure 7. Number of panels that fail within the range of each bin in the case of no maintenance process.

average number of maintenance stops reduces to nearly one for both PdM and PdM-skip. On the other hand, the longer the forward prediction interval is, the more prediction uncertainty will be involved, resulting in an increase of the number of repaired panels. In summary, a longer prediction interval will reduce the number of maintenance stops while increasing the number of repaired panels, and vice versa. For example, based on our experience, when the forward prediction interval in PdM-skip decreases to 4000, the average number of maintenance stops increases to 3.1 while the average number of repaired panels decreases to 7.62 (i.e. 762 repaired panels for the whole fleet). Therefore, in reality, the number of maintenance stops and the number of repaired panels can be traded off by tuning the prediction interval, depending on the cost of one maintenance stop and the cost of repairing one panel. If the cost of one maintenance stop was much higher than that of repairing one panel, one would tend to repair more panels once a maintenance stop is triggered. In this case, it would be cheaper to use a long prediction interval in the trade off between the number of repaired panels and the number of maintenance stops. In contrast, if the cost of repairing one panel was more significant than that of one maintenance stop, then a shorter prediction interval would make more sense.

We now discuss further the two prognostics-based strategies. PdM is designed completely independently without considering the time of scheduled maintenance (Figure 5). All the stops were unscheduled maintenance that occurred outside the time of scheduled maintenance. In PdM-skip, all the maintenance stops occurred during one of the 10 scheduled maintenance stops. The results indicate that PdM-skip fits well the objective that it ensures as much as possible that maintenance activities are carried out during the time of scheduled maintenance and this turns out indeed to be more economical from a maintenance cost point of view.

Figures 7–9 illustrate the statistical character of the number of failed/repaired panels over the entire fleet, that is, 100×500 panels. The histogram of the failure

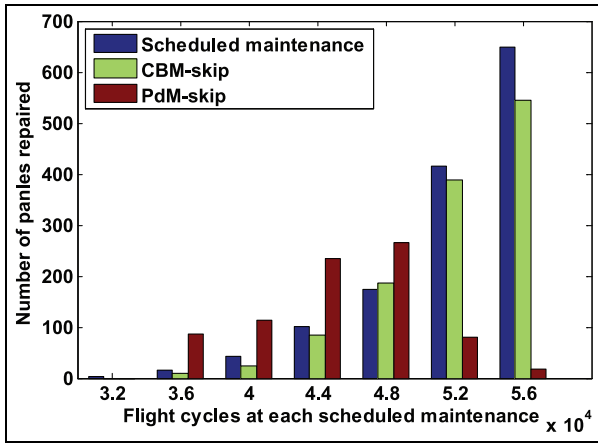


Figure 8. Comparison of maintenance strategies in terms of the number of repaired panels at scheduled maintenance stops. The first three scheduled stops are not plotted.

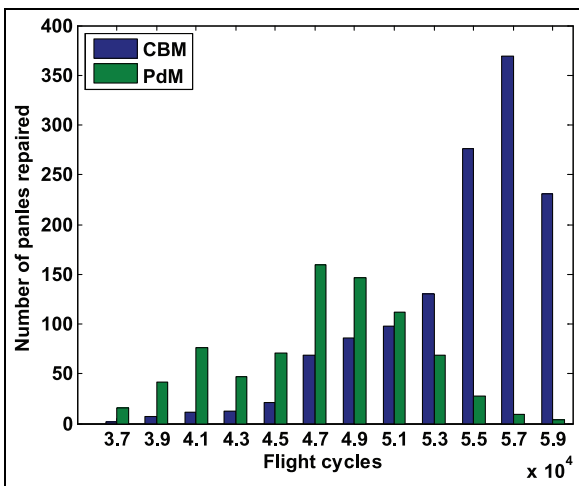


Figure 9. Comparison of CBM and PdM in terms of number of repaired panels within the time range of each bin.

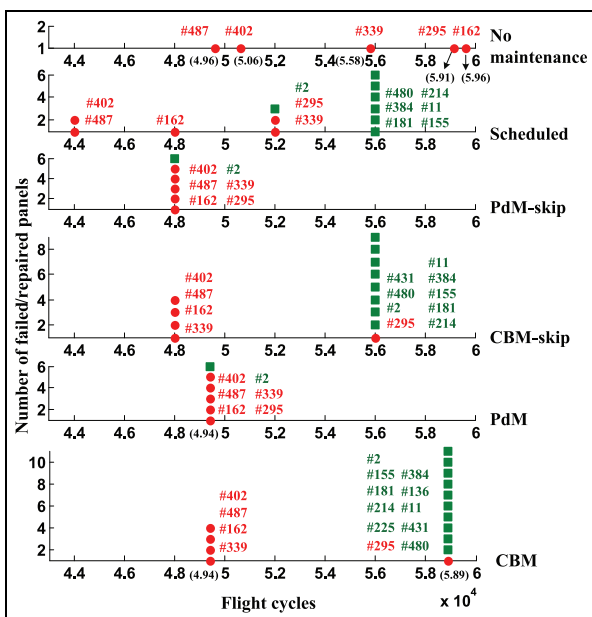


Figure 10. Different processes for aircraft #30.

time in the case of no maintenance intervention is given in Figure 7. The numbers in the x -axis are the center of the bin and the bin width is 2000 cycles. For example, the first bin means that there are two panels whose failure time are within the range of [36000,38000]. We see that most failures occur in the second half of the lifetime and the number of failed panels gradually increases toward the EOL.

Figure 8 compares the scheduled maintenance, CBM-skip, and PdM-skip strategies in terms of the number of repaired panels at scheduled stops (recall that there are 10 scheduled stops, see Figure 5). The first three scheduled stops are not plotted because no panels were repaired at the first three stops in all strategies. This shows that PdM-skip reduced by nearly 80% the “unnecessary repair” compared to CBM-skip, since PdM-skip decreases the conservativeness level by doing prognostics for each panel. The panels that are repaired in CBM-skip may not be necessary to be repaired in PdM-skip due to their slow growth rates, thus not threatening safety. One may note that PdM-skip repaired more panels than CBM-skip in the earlier stage of the aircraft lifetime. It is because once the maintenance is requested, PdM-skip performs a long horizon prediction. Therefore, the panels that might exceed the threshold in the later stage are repaired in advance. Once a panel is repaired, the crack is assumed to re-grow from a small initial crack size. The probability that this panel is repaired again during the aircraft lifetime is negligible.

Figure 9 compares CBM and PdM in terms of the number of repaired panels within the time range of each bin. The figure shows that PdM significantly reduces the number of repaired panels, and most of the panels are repaired at an earlier period of the aircraft lifetime due to a long forward prediction interval. CBM repairs many cracks slightly larger than the repair threshold near the EOL, but actually these panels do not affect safety. In contrast, PdM reduces this “unnecessary repair” by considering the future reliability.

In order to give more insight of the dynamics of the six processes, i.e., no maintenance, scheduled maintenance, PdM-skip, CBM-skip, PdM, and CBM, we take the simulation results of aircraft no.30 as an example. The results are illustrated in Figure 10. The specific cycle at which one or more specific panels are repaired are shown in Figure 10. The symbol “#” represents the panel index. The numbers in parentheses along the x -axis in subplots 1, 5, and 6 are the cycles corresponding to the failure/repair in the process of no maintenance intervention, CBM, and PdM, respectively. For example, in subplot 1, Panel 487 fails at 49,600th cycle. The red solid dots and the green solid squares along the y -axis represent the “actually failed” panels and the “unnecessarily repaired” panels, respectively. It can be seen that all the “actually failed” panels shown in the first subplot are repaired in all other maintenance processes prior to their failure, that is to say, all maintenance strategies ensure safety. CBM wastes many

panels near the EOL while PdM-skip and PdM have the least unnecessary repair.

In order to further assess the effectiveness of prognostics-based maintenance over threshold-based maintenance in different situations, we also studied the six maintenance strategies while considering a smaller panel-to-panel uncertainty, that is, a smaller uncertainty in material properties $\{m, C\}$ and in the pressure differential p . This was implemented by reducing the coefficient of variance of $\{m, C\}$ and p in Table 2 to 0.5% while keeping other values unchanged. We found that prognostics-based strategies (PdM and PdM-skip) gain slightly over the threshold-based ones (CBM and CBM-skip) in terms of repaired panels in the small uncertainty case, while they more significantly outperform the threshold-based strategies when larger uncertainties are present. This is caused by the different philosophies of these two types of strategies. The prognostics-based strategies repair a panel based on its individual crack growth behavior while the threshold-based ones have the same repair threshold for all panels. Specifically, when the uncertainties in material property parameters $\{m, C\}$ and in pressure p are small, both the panel-to-panel variability and the variability present in the crack propagation process are small, leading the cracks in the panels to have similar propagation behavior. In this situation, the two types of strategies have similar performance. In contrast, when large uncertainties are present in $\{m, C\}$ and p , the cracks have large variability in propagation rate among the panel population. In the threshold-based strategies, due to the constant repair threshold, all panels with a crack size greater than the repair threshold are repaired, even if some of them have a very low growth rate and are not likely to fail until the aircraft's EOL. Prognostics-based strategies have an advantage in this situation since they treat the panels individually. Combined with the crack size and the material property parameters of each panel at the current time, PdM/PdM-skip predicts its crack growth trajectory in a future period and makes the decision of whether to replace this panel based on this predicted behavior.

Conclusion

In the context of fatigue crack growth in fuselage panels, where material properties and initial crack sizes are unknown, and the cabin pressure differential is random, we considered a newly developed model-based prognostics method. Based on that, we proposed two prognostics-based strategies for the maintenance of aircraft fuselage panels, PdM and PdM-skip. PdM and PdM-skip are compared with the traditional scheduled maintenance and two other threshold-based strategies, that is, CBM/CBM-skip proposed in Pattabhiraman et al.,¹ through simulated application to a fleet of short-range commercial aircraft. A cost model is used to quantify and compare the cost-effectiveness of different

strategies. It is found that PdM/PdM-skip gained significantly over scheduled maintenance and CBM/CBM-skip because future reliability is calculated individually for each panel, and incorporated into maintenance decision-making. In comparing the two prognostics-based strategies, all PdM maintenance stops occurred as unscheduled maintenance, which is more expensive due to less advance notice, while almost all PdM-skip maintenance stops happened at scheduled maintenance.

Note that due to the Gaussian assumption of the EKF, the crack size is assumed normally distributed throughout all the stages, which may not always be accurate. This assumption could be relaxed by choosing some non-Gaussian filter methods instead of the EKF. The FOP method could also be extended to adapt to the non-Gaussian assumption on crack size distribution.

Further note that the proposed maintenance strategies involve some user-defined parameters that affect their final cost-effectiveness. We carried out basic trade-off studies to decide on the values of these parameters but more comprehensive approaches could be considered as part of future work: (1) within the current framework, all these parameters could be optimized simultaneously for minimum average maintenance cost over the entire fleet and (2) the framework could be reformulated to consider only parameters that have objectively set values. For example, the maintenance approaches could be reformulated such as to only depend on the costs of scheduled and unscheduled maintenance. The cost ratio of scheduled over unscheduled maintenance turns out to be a major driver of the maintenance decisions. A first study aimed at defining optimal prognostics-based strategies for a given cost ratio has been considered in Wang et al.²⁰ using simpler maintenance models. Extending such strategies to the more complex maintenance models considered here would also represent an interesting line of future work.

Declaration of conflicting interests

The author(s) declared no potential conflicts of interest with respect to the research, authorship, and/or publication of this article.

Funding

The author(s) received no financial support for the research, authorship, and/or publication of this article.

References

1. Pattabhiraman S, Gogu C, Kim NH, et al. Skipping unnecessary structural airframe maintenance using an on-board structural health monitoring system. *Proc IMechE, Part O: J Risk and Reliability* 2012; 226: 549–560.
2. Xiaoliang Z, Huidong G, Guangfan Z, et al. Active health monitoring of an aircraft wing with embedded piezoelectric sensor/actuator network: I. Defect detection, localization and growth monitoring. *Smart Mater Struct* 2007; 16: 1208.

3. Ignatovich SR, Menou A, Karuskevich MV, et al. Fatigue damage and sensor development for aircraft structural health monitoring. *Theor Appl Fract Mec* 2013; 65: 23–27.
4. Diamanti K and Soutis C. Structural health monitoring techniques for aircraft composite structures. *Prog Aerosp Sci* 2010; 46: 342–352.
5. Jeong-Beom I and Fu-Kuo C. Detection and monitoring of hidden fatigue crack growth using a built-in piezoelectric sensor/actuator network: I. Diagnostics. *Smart Mater Struct* 2004; 13: 609.
6. Deloux E, Castanier B and Bérenguer C. Maintenance policy for a deteriorating system evolving in a stressful environment. *Proc IMechE, Part O: J Risk and Reliability* 2008; 222: 613–622.
7. Huynh KT, Barros A and Berenguer C. Adaptive condition-based maintenance decision framework for deteriorating systems operating under variable environment and uncertain condition monitoring. *Proc IMechE, Part O: J Risk and Reliability* 2012; 226: 602–623.
8. Wang W, Hussin B and Jefferis T. A case study of condition based maintenance modelling based upon the oil analysis data of marine diesel engines using stochastic filtering. *Int J Prod Econ* 2012; 136: 84–92.
9. Wang HK, Huang HZ, Li YF, et al. Condition-based maintenance with scheduling threshold and maintenance threshold. *IEEE T Reliab* 2016; 65: 513–524.
10. Huynh KT, Barros A and Berenguer C. Multi-level decision-making for the predictive maintenance of k-out-of-n: F deteriorating systems. *IEEE T Reliab* 2015; 64: 94–117.
11. Huynh KT, Barros A and Berenguer C. Maintenance decision-making for systems operating under indirect condition monitoring: value of online information and impact of measurement uncertainty. *IEEE T Reliab* 2012; 61: 410–425.
12. Deloux E, Castanier B and Bérenguer C. Predictive maintenance policy for a gradually deteriorating system subject to stress. *Reliab Eng Syst Safe* 2009; 94: 418–431.
13. Curcurù G, Galante G and Lombardo A. A predictive maintenance policy with imperfect monitoring. *Reliab Eng Syst Safe* 2010; 95: 989–997.
14. Van Horenbeek A and Pintelon L. A dynamic predictive maintenance policy for complex multi-component systems. *Reliab Eng Syst Safe* 2013; 120: 39–50.
15. Nguyen K-A, Do P and Grall A. Multi-level predictive maintenance for multi-component systems. *Reliab Eng Syst Safe* 2015; 144: 83–94.
16. Lorton A, Fouladirad M and Grall A. Computation of remaining useful life on a physic-based model and impact of a prognosis on the maintenance process. *Proc IMechE, Part O: J Risk and Reliability* 2013; 227: 434–449.
17. Langeron Y, Grall A and Barros A. A modeling framework for deteriorating control system and predictive maintenance of actuators. *Reliab Eng Syst Safe* 2015; 140: 22–36.
18. Liu J, Zhang M, Zuo H, et al. Remaining useful life prognostics for aeroengine based on superstatistics and information fusion. *Chinese J Aeronaut* 2014; 27: 1086–1096.
19. Jardine AKS, Lin D and Banjevic D. A review on machinery diagnostics and prognostics implementing condition-based maintenance. *Mech Syst Signal Pr* 2006; 20: 1483–1510.
20. Wang Y, Gogu C, Binaud N, et al. A cost driven predictive maintenance policy for structural airframe maintenance. *Chinese J Aeronaut* 2017; 30: 1242–1257.
21. Paris P and Erdogan F. A critical analysis of crack propagation laws. *J Basic Eng: T ASME* 1963; 85: 528–533.
22. Tanaka K, Masuda C and Nishijima S. The generalized relationship between the parameters C and m of Paris' law for fatigue crack growth. *Scripta Metall Mater* 1981; 15: 259–264.
23. Molent L and Barter SA. A comparison of crack growth behaviour in several full-scale airframe fatigue tests. *Int J Fatigue* 2007; 29: 1090–1099.
24. Karandikar JM, Kim NH and Schmitz TL. Prediction of remaining useful life for fatigue-damaged structures using Bayesian inference. *Eng Fract Mech* 2012; 96: 588–605.
25. Gobbato M, Kosmatka JB and Conte JP. A recursive Bayesian approach for fatigue damage prognosis: an experimental validation at the reliability component level. *Mech Syst Signal Pr* 2014; 45: 448–467.
26. Sun J, Zuo H, Wang W, et al. Prognostics uncertainty reduction by fusing on-line monitoring data based on a state-space-based degradation model. *Mech Syst Signal Pr* 2014; 45: 396–407.
27. Doucet A and Johansen AM. A tutorial on particle filtering and smoothing: Fifteen years later. *Handb Nonlinear Filter* 2009; 12: 656–704.
28. Roblès B, Avila M, Duculty F, et al. Hidden Markov model framework for industrial maintenance activities. *Proc IMechE, Part O: J Risk and Reliability* 2014; 228: 230–242.
29. Le TT, Chatelain F and Bérenguer C. Multi-branch hidden Markov models for remaining useful life estimation of systems under multiple deterioration modes. *Proc IMechE, Part O: J Risk and Reliability* 2016; 230: 473–484.
30. Saxena A, Celaya J, Saha B, et al. On applying the prognostic performance metrics. In: *Processings of the annual conference of the prognostics and health management society*, San Francisco, CA, 27 September–1 October, 2009. https://www.phmsociety.org/sites/phmsociety.org/files/p hm_submission/2009/phmc_09_39.pdf
31. Kale AA and Haftka RT. Tradeoff of weight and inspection cost in reliability-based structural optimization. *J Aircraft* 2008; 45: 77–85.
32. Kundu AK. *Aircraft design*. Cambridge: Cambridge University Press, 2010.
33. Kim NH, An D and Choi J-H. *Prognostics and health management of engineering systems, an introduction*. Cham: Springer International Publishing, 2017, p.347.
34. Cortie MB and Garrett GG. On the correlation between the C and m in the paris equation for fatigue crack propagation. *Eng Fract Mech* 1988; 30: 49–58.
35. Bilir ÖG. The relationship between the parameters C and n of Paris' law for fatigue crack growth in a SAE 1010 steel. *Eng Fract Mech* 1990; 36: 361–364.
36. Rice JA. *Mathematical statistics and data analysis*. Scarborough, ON: Nelson Education, 2006.
37. Huang B and Du X. Probabilistic uncertainty analysis by mean-value first order saddlepoint approximation. *Reliab Eng Syst Safe* 2008; 93: 325–336.
38. Grewal MS and Andrews AP. *Kalman filtering: theory and practice with MATLAB*. 4th ed. Mississauga, ON: Wiley-Interscience, 2014.
39. Wang Y, Binaud N, Gogu C, et al. Determination of Paris' law constants and crack length evolution via

extended and unscented Kalman filter: an application to aircraft fuselage panels. *Mech Syst Signal Pr* 2016; 80: 262–281.

40. Wang Y, Gogu C, Binaud N, et al. *Predicting remaining useful life by fusing SHM data based on extended Kalman filter: safety and reliability of complex engineered systems*. Boca Raton, FL: CRC Press, 2015, pp.2489–2496.

Appendix I

Model the degradation process as a hidden Markov model

The Euler method is used to solve the differential equation of equation (1) with a discrete step size of one. The discrete Paris model is written in a recursive form given in equation (7)

$$a_k = a_{k-1} + C \left(A \frac{p_{k-1}^r}{t} \sqrt{\pi a_{k-1}} \right)^m = g(a_{k-1}, p_{k-1}) \quad (7)$$

We model the pressure differential p as a random variable that varies at every flight cycle. At cycle k , p is modeled as

$$p_k = \bar{p} + \Delta p_k \quad (8)$$

where \bar{p} is the average pressure differential and Δp_k is the pressure disturbance. The disturbance around the average pressure is modeled as a normally distributed random variable with zero mean and variance σ_p^2 . Since uncertainty in the pressure differential is generally small, a mean-value first-order second moment (MVFOSM) approach³⁷ is used here. Then equation (7) can be written as

$$a_k = g(a_{k-1}, \bar{p}) + \frac{\partial g(a_{k-1}, \bar{p})}{\partial p} \Delta p_{k-1} \quad (9)$$

in which $(\partial g(a_{k-1}, \bar{p})/\partial p)\Delta p_{k-1}$ is seen as the additive process noise. By considering that \bar{p} is a constant, equation (9) becomes

$$a_k = f(a_{k-1}) + w_{k-1} \quad (10)$$

where $f(a_{k-1}) = g(a_{k-1}, \bar{p})$ and

$$w_{k-1} = (\partial f(a_{k-1})/\partial p)\Delta p_{k-1} \quad (11)$$

Given that Δp_{k-1} is normally distributed and $\partial f(a_{k-1})/\partial p$ is constant, the additive process noise w_k follows a normal distribution with mean zero and variance Q_k , which is calculated analytically by equation (12)

$$\begin{aligned} Q_k &= \left(\frac{\partial g(a_k, \bar{p})}{\partial p} \sigma_p \right)^2 \\ &= \left(C m (A r / t)^m (\bar{p})^{m-1} (\pi a_k)^{m/2} \sigma_p \right)^2 \end{aligned} \quad (12)$$

The noisy measurement data are simulated using equation (13), in which a_k is the crack size at k th cycle and v_k the measurement noise

$$z_k = a_k + v_k \quad (13)$$

Equations (10) and (13) are the state equation and the measurement equation of the hidden Markov model, respectively. In terms of state-parameter estimation using extended Kalman filter (EKF), it defines the parameter vector as an additional state variable and artificially appends it onto the true state vector to form a single joint state vector and estimate the state and parameters simultaneously. In the aforementioned crack growth model, m and C are the unknown parameters that need to be estimated. Therefore, a two-dimensional parameter vector is defined as

$$\Theta = [m, C]^T \quad (14)$$

Appending Θ to the state variable, the augmented state vector is then defined in equation (15)

$$\mathbf{x}_{\text{au}} = [a \ m \ C]^T \quad (15)$$

EKF is used as a black box and the details of the algorithm will not be presented here. Readers could refer to the literature^{38,39} for a general introduction and to Wang et al.⁴⁰ for its implementation to fatigue damage state estimation. By applying EKF, at cycle k , the a posteriori estimation of the augmented state vector, denoted by $\mathbf{x}_{\text{au},k}$, and the corresponding covariance matrix \mathbf{P}_k can be obtained.

Details of first-order perturbation method

Suppose the current flight cycle is S . According to the EKF, the state vector $\mathbf{x}_{\text{au},S}$ is multivariate normally distributed with mean $\hat{\mathbf{x}}_{\text{au},S}$ and covariance \mathbf{P}_S , presented as

$$\mathbf{x}_{\text{au},S} \sim N(\hat{\mathbf{x}}_{\text{au},S}, \mathbf{P}_S) \quad (16)$$

Let us define

$$f_L(a, m, C, p) = C \left(A \frac{p^r}{t} \sqrt{\pi a} \right)^m \quad (17)$$

The Paris model is then written as

$$a_k = a_{k-1} + f_L(a_{k-1}, m, C, p_{k-1}) \quad (18)$$

Note that the time index k starts from $S + 1$ and goes up to $S + h$, where h is the number of flight cycles forward one wants to predict. In the stochastic process, the “expected trajectory” is the particular solution when the involved random variables are taken as their expected values. For the problem discussed at hand, the “expected trajectory” of the crack size is the sequence $\{\bar{a}_k | k = S + 1, S + 2, \dots, S + h\}$ obtained as a solution of equation (19), with zero process noise and with the expected value $\bar{a}_S, \bar{m}, \bar{C}$, and \bar{p} as the initial values of the corresponding random variables. Note that the symbol “ $-$ ” denotes the expected value of a random variable

$$\bar{a}_k = \bar{a}_{k-1} + f_L(\bar{a}_{k-1}, \bar{m}, \bar{C}, \bar{p}) \quad (19)$$

Due to the presence of uncertainties and the random noise, a_k , m , C , and p_k are modeled by adding a perturbation to their expected values. Let the symbol “ Δ ” denotes the perturbation; then a_k , m , C , and p_k can be written as

$$a_k = \bar{a}_k + \Delta a_k \quad (20)$$

$$m = \bar{m} + \Delta m \quad (21)$$

$$C = \bar{C} + \Delta C \quad (22)$$

$$p_k = \bar{p} + \Delta p_k \quad (23)$$

Δp_k is related to the cabin pressure differential that varies from cycle to cycle while Δm and ΔC are uncertainties related to panel materials and thus do not vary with time. The available information at $k = S$, as given in equations (24) and (25), will be used as the initial condition in the following derivation

$$[\bar{a}_S, \bar{m}, \bar{C}]^T = [\hat{a}_S, \hat{m}_S, \hat{C}_S]^T \quad (24)$$

$$[\Delta a_S, \Delta m, \Delta C]^T \sim N(\mathbf{0}_{3 \times 1}, \mathbf{P}_S) \quad (25)$$

By subtracting equation (19) from equation (18), the perturbation of a_k is obtained as

$$\Delta a_k = \Delta a_{k-1} + f_L(a_{k-1}, m, C, p_{k-1}) - f_L(\bar{a}_{k-1}, \bar{m}, \bar{C}, \bar{p}) \quad (26)$$

The first-order approximation is used. Defining $\boldsymbol{\lambda}_{k-1} = [\bar{a}_{k-1}, \bar{m}, \bar{C}, \bar{p}]$, which is a known vector, equation (26) reduces to

$$\begin{aligned} \Delta a_k = \Delta a_{k-1} + \frac{\partial f_L(\boldsymbol{\lambda}_{k-1})}{\partial a} \Delta a_{k-1} + \frac{\partial f_L(\boldsymbol{\lambda}_{k-1})}{\partial m} \\ + \frac{\partial f_L(\boldsymbol{\lambda}_{k-1})}{\partial C} \Delta C + \frac{\partial f_L(\boldsymbol{\lambda}_{k-1})}{\partial p} \Delta p_{k-1} \end{aligned} \quad (27)$$

The following substitution is done to simplify equation (27)

$$L_{k-1} = 1 + \frac{\partial f_L(\boldsymbol{\lambda}_{k-1})}{\partial a} \quad (28)$$

$$M_{k-1} = \frac{\partial f_L(\boldsymbol{\lambda}_{k-1})}{\partial m} \quad (29)$$

$$N_{k-1} = \frac{\partial f_L(\boldsymbol{\lambda}_{k-1})}{\partial C} \quad (30)$$

$$w_{k-1}^L = \frac{\partial f_L(\boldsymbol{\lambda}_{k-1})}{\partial p} \Delta p_{k-1} \quad (31)$$

in which w_{k-1}^L is the random noise with mean zero and standard deviation σ_{k-1} , which can be calculated by equation (32). Here, w_i^L and w_j^L ($i \neq j$) are considered independent

$$\sigma_{k-1} = \frac{\partial f_L(\boldsymbol{\lambda}_{k-1})}{\partial p} \sigma_p \quad (32)$$

Then equation (27) becomes

$$\Delta a_k = L_{k-1} \Delta a_{k-1} + M_{k-1} \Delta m + N_{k-1} \Delta C + w_{k-1}^L \quad (33)$$

The following derivation is for calculating the uncertainty structure of Δa_k . Rewrite equation (33) as the

function of the initial value, that is, $[\Delta a_S \Delta m, \Delta C]$, then after k time iterations, Δa_k can be written as equation (34), in which we use A_k , B_k , and D_k to represent the coefficient of Δa_S , Δm , and ΔC , respectively, and E_k to denote the noise term

$$\Delta a_k = A_k \Delta a_S + B_k \Delta m + D_k \Delta C + E_k \quad (34)$$

In equation (34), Δa_S , Δm , and ΔC are stationary random variables whose probability distributions do not change when shifted in time. A_k , B_k , and D_k are deterministic and evolve with time and are calculated recursively with their initial values A_S , B_S , C_S , as shown in equations (35)–(37). E_k is a non-stationary random variable whose distribution varies with time and is derived recursively by equation (38). Since E_k is a linear combination of independent and identically distributed random variables, it is itself a normal variable such that $E_k \sim N(0, F_k)$. F_k is calculated by the recursive expression given in equation (39). Note that w_k^L and σ_k in equations (38) and (39) refer to equations (31) and (32), respectively

$$A_k = L_k A_{k-1} \quad (35)$$

$$B_k = L_k B_{k-1} + M_k \quad (36)$$

$$D_k = L_k D_{k-1} + N_k \quad (37)$$

$$E_k = L_k E_{k-1} + w_k^L \quad (38)$$

$$F_k = L_k^2 F_{k-1} + \sigma_k^2 \quad (39)$$

Provided that Δa_S , Δm , ΔC , and E_k are random variables, and that A_k , B_k , D_k are deterministic, equation (34) is rewritten as matrix form such that $\Delta a_k = \mathbf{B}_k \boldsymbol{\beta}_k$, in which $\mathbf{B}_k = [A_k, B_k, D_k, 1]$ and $\boldsymbol{\beta}_k = [\Delta a_S, \Delta m, \Delta C, E_k]^T$. Considering that $[\Delta a_S, \Delta m, \Delta C]^T \sim N(\mathbf{0}_{3 \times 1}, \mathbf{P}_S)$ and $E_k \sim N(0, F_k)$, $\boldsymbol{\beta}_k$ is a multivariate normal vector such that $\boldsymbol{\beta}_k \sim N(\boldsymbol{\mu}, \boldsymbol{\Sigma})$, in which $\boldsymbol{\mu} = [\mathbf{0}_{4 \times 1}]$ and $\boldsymbol{\Sigma} = \text{diag}(\mathbf{P}_S, F_k)$. According to the theory of affine transformation of multivariate Gaussian random variables, Δa_k is normally distributed such that $\Delta a_k \sim N(\mathbf{B}_k \boldsymbol{\mu}, \mathbf{B}_k \boldsymbol{\Sigma} \mathbf{B}_k^T)$, in which

$$\mathbf{B}_k \boldsymbol{\mu} = 0 \quad (40)$$

$$\mathbf{B}_k \boldsymbol{\Sigma} \mathbf{B}_k^T = [A_k, B_k, D_k] \mathbf{P}_S [A_k, B_k, D_k]^T + F_k \quad (41)$$

Given that $a_k = \bar{a}_k + \Delta a_k$ and \bar{a}_k is deterministic, a_k is a normal variable that $a_k \sim N(\mu_{ak}, \sigma_{ak})$, in which

$$\mu_{ak}^F = \bar{a}_k \quad (42)$$

$$\sigma_{ak}^F = \sqrt{\mathbf{B}_k \boldsymbol{\Sigma} \mathbf{B}_k^T} \quad (43)$$

The superscript “F” stands for first-order perturbation (FOP) method in order to distinguish the Monte Carlo (MC) simulation that will be presented in Appendix 2. Equations (42) and (43) enable to compute analytically the crack size distribution from cycle $S + 1$ to cycle $S + h$.

Table 4. Initial conditions for the 10 picked panels.

No.	a_0 (mm)	m	C	Corresponding service life (cycles)
1	0.45	3.8	1.87E-10	52,700
2	0.61	3.7	1.95E-10	51,300
3	0.58	3.8	1.86E-10	45,000
4	0.44	3.7	1.98E-10	59,300
5	0.61	3.7	1.92E-10	46,700
6	0.59	3.6	2.03E-10	58,700
7	0.46	3.8	1.86E-10	58,800
8	0.54	3.7	1.98E-10	57,600
9	0.47	3.7	1.90E-10	59,400
10	0.50	3.7	1.96E-10	57,300

Appendix 2

Performance comparison between FOP method and MC simulation

We verify the accuracy of the proposed FOP method by comparing it with MC simulation. According to section “Results and discussion,” if no maintenance is carried out, there are 692 failed panels, that is, the crack sizes on these 692 panels exceed the critical threshold a_{cr} before the end of the aircraft lifetime (60,000 cycles). Failed panels imply faster crack growth rates and strongly nonlinear crack growth curves. In contrast, the non-failed panels indicate that the cracks maintain a moderate or very low growth rate, and thus, the crack growth curves show modest nonlinearity during the whole lifetime of the aircraft. If the FOP method performs well in the strongly nonlinear crack growth process (corresponding to the failed panels), then it should also maintain reasonably good efficacy for the minor nonlinear cases (non-failed panels). Therefore, we investigate only the accuracy of the FOP method on the failed panels. Due to limitations of space, we chose randomly 10 panels from the 692 failed panels to present the results quantitatively.

The initial conditions of these 10 panels, i.e., the initial crack size a_0 , the true m and C are reported in Table 4. The last column is the service life of each panel. It is noted that the service life of one panel is the accumulated flight cycles of the panel right before the crack size exceeds the critical threshold $a_{cr} = 59.6$ mm. The service life of the i th panel is denoted by Li .

For each of the critical panels, we predict the evolution of the crack size distribution using FOP method and MC simulation in the last J cycles prior to the end of the service life of each panel. This validates the FOP method since we deal with the most nonlinear part of the crack growth curve. The evolution of the distribution given by FOP is compared with that given by MC simulation to investigate the performance of FOP method. The details for implementing the comparison are elaborated as follows:

1. For the i th panel ($i = 1, 2, \dots, 10$), apply the EKF to carry out the state-parameter estimation from cycle $k = 1$ until $k = Li - J$. The estimated state

vector and the covariance matrix at $k = Li - J$ are denoted as $\hat{\mathbf{x}}_{au, Li-J}$ and \mathbf{P}_{Li-J} .

2. From $k = Li - J + 1$ to $k = Li$ (i.e. the last J cycles), predict the mean μ_{ak}^F (see equation (42)) and standard deviation σ_{ak}^F (see equation (43)) of the crack size using FOP method (see Appendix 1 for details).
3. From $k = Li - J + 1$ to $k = Li$ (i.e. the last J cycles), predict the mean and the standard deviation of the crack size using MC simulation. Specifically, generate N_s samples at $k = Li - J$ based on $\hat{\mathbf{x}}_{au, Li-J}$ and \mathbf{P}_{Li-J} , that is, sample $\mathbf{x}_{au, Li-J}^j \sim N(\hat{\mathbf{x}}_{au, Li-J}, \mathbf{P}_{Li-J})$ ($j = 1, 2, \dots, N_s$). Propagate forward each sample from $k = Li - J + 1$ to $k = Li$ through equation (10) and then at cycle k , the mean and standard deviation, denoted by μ_{ak}^M and σ_{ak}^M , can be calculated from the N_s samples.

According to the nature of the EKF-FOP method, the crack size is normally distributed characterized by mean and standard deviation. Therefore, comparing the crack size distribution predicted by FOP and MC methods is equivalent to comparing μ_{ak}^F and μ_{ak}^M , σ_{ak}^F and σ_{ak}^M ($k = Li - J + 1, Li - J + 2, \dots, Li$).

The relative error between μ_{ak}^F and μ_{ak}^M , σ_{ak}^F and σ_{ak}^M are calculated as follows, $e_{\mu k} = |\mu_{ak}^F - \mu_{ak}^M| / \mu_{ak}^M$, $e_{\sigma k} = |\sigma_{ak}^F - \sigma_{ak}^M| / \sigma_{ak}^M$ ($k = Li - J + 1, Li - J + 2, \dots, Li$). The relative error increases as cycles increase. We present in Table 5 the maximum value of $e_{\mu k}$ and $e_{\sigma k}$, which are obtained at the end of the service life ($k = Li$) of each panel. The first column is the index of the panel whose initial condition and the corresponding service life have been presented in Table 4. One may note that the true crack size at the end of the service life of each panel is smaller than the critical threshold $a_{cr} = 59.6$ mm. That is because the crack size grows very fast in the stage near the threshold and exceeds a_{cr} in the next maintenance assessment interval (100 cycles).

We draw the following conclusions based on the results. (1) The FOP method gives very close results to that of MC with maximal relative error 1.26% for the mean (Panel 1) and 3.51% for the standard deviation (Panel 1). (2) For Panels 8, 9, and 10, the mean of the crack size estimated by FOP is a bit underestimated (i.e. smaller than the true crack size). However, when

Table 5. Comparison of the mean and standard deviation of the crack size given by FOP and MC simulation at the end of the service life ($k=L_i$) of each panel.

No.	μ_{ak}^F (mm)	μ_{ak}^M (mm)	$e_{\mu k}$ (%)	σ_{ak}^F (mm)	σ_{ak}^M (mm)	$e_{\sigma k}$ (%)	True crack size (mm)	95% CI based on μ_{ak}^F and σ_{ak}^F (mm)
1	58.08	58.83	1.26	7.75	8.03	3.51	55.94	[42.89, 73.28]
2	60.00	60.19	0.31	4.42	4.55	2.76	58.50	[51.33, 68.67]
3	62.68	63.29	0.96	7.88	8.13	3.14	56.65	[47.25, 78.12]
4	56.02	56.30	0.49	5.29	5.30	0.11	54.78	[45.65, 66.39]
5	54.96	55.20	0.42	4.66	4.81	3.01	53.91	[45.83, 64.10]
6	59.26	59.39	0.22	3.37	3.44	2.05	59.18	[52.66, 65.86]
7	60.13	60.55	0.69	6.08	6.27	3.01	59.57	[48.22, 72.04]
8	55.68	55.78	0.18	3.71	3.74	0.78	55.74	[48.41, 62.95]
9	54.09	54.23	0.26	4.59	4.65	1.17	54.19	[45.09, 63.08]
10	56.48	56.57	0.16	4.77	4.85	1.66	56.62	[47.12, 65.83]

Table 6. The five metrics for the 10 panels.

Panel no.	PH ($\alpha = 0.1$)	$\alpha - \lambda$ accuracy ($\alpha = 0.1, \lambda = 0.5$)	RA	CRA	Convergence
1	52,500	True	0.93	0.97	21,248
2	47,500	False	0.99	0.98	9445
3	38,100	True	0.94	0.94	11,096
4	49,900	True	0.96	0.93	13,936
5	37,800	True	0.99	0.93	12,618
6	50,700	False	0.95	0.86	8894
7	51,900	False	0.95	0.92	10,703
8	43,400	False	0.98	0.93	14,592
9	48,700	False	0.97	0.91	11,355
10	46,500	False	0.93	0.86	11,388

PH: prognostics horizon; RA: relative accuracy; CRA: cumulative relative accuracy.

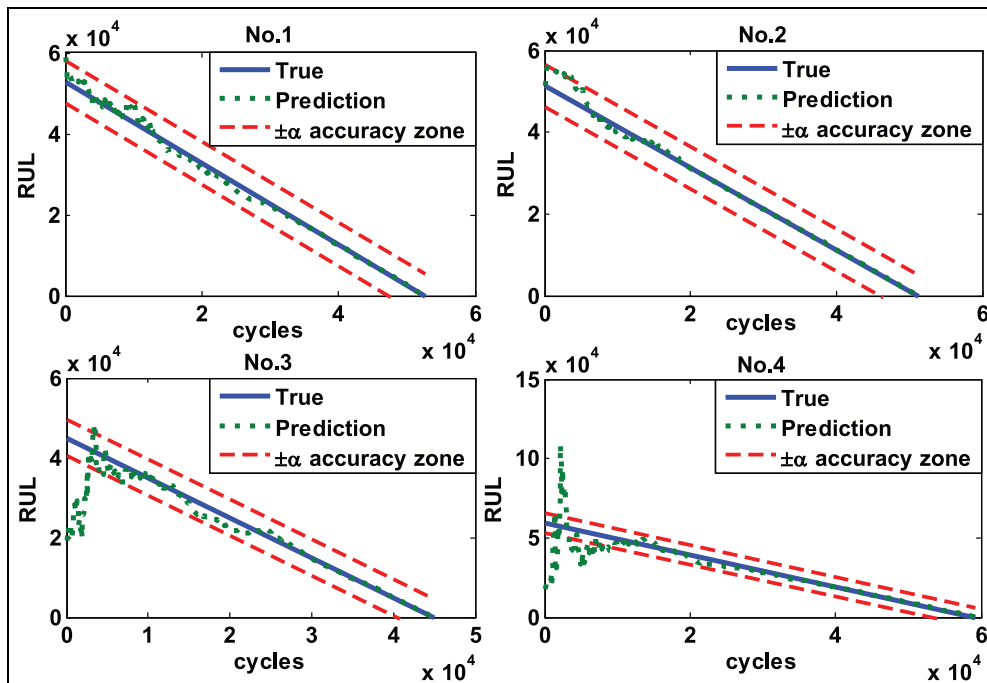


Figure 11. PH with $\alpha = 0.1$ of Panels 1–4.

considering the 95% confidence interval, the prediction remains conservative. The last column presents all the 95% confidence interval of the predicted mean. (3) The processing time of predicting one crack growth in one panel is 0.006 s (FOP) versus 29 s (MC) on a laptop

with a processor Intel(R) Core(TM) i5-3337U CPU 1.8 GHz. This computational saving is significantly meaningful to the predictive maintenance since the maintenance strategies are applied to an aircraft fleet containing thousands of panels.

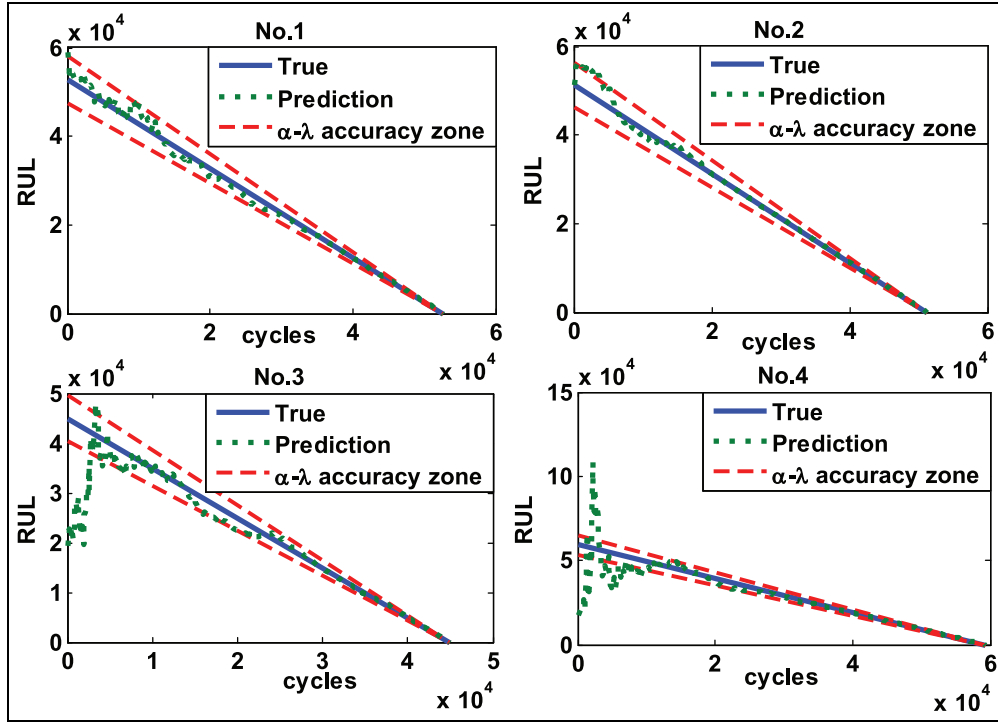


Figure 12. $\alpha - \lambda$ accuracy with $\alpha = 0.1$ and $\lambda = 0.5$ of Panels 1–4.

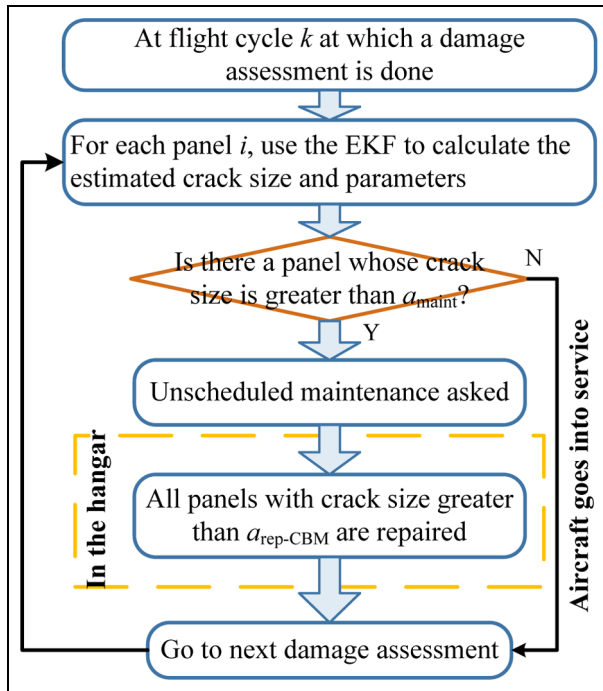


Figure 13. Flowchart of CBM.

Appendix 3

Evaluating the prognostics method by prognostics metrics

The proposed prognostics method is further evaluated by comparing with true known remaining useful life (RUL) using five established prognostics metrics:³⁰ prognostics horizon (PH), $\alpha - \lambda$ accuracy, relative accuracy

(RA), cumulative relative accuracy (CRA), and convergence. Readers refer to the literature^{30,33} for detailed information about the five metrics. It is noted that these metrics are possible only when the true RUL is available.

We continue to use the 10 panels that were randomly picked from the 692 failed panels in Appendix 2 to verify the proposed prognostics method. The service life of each panel is listed in Table 4, which is used to obtain the true RUL. The predicted RUL is computed each time when a new measurement arrives and the state-parameter is carried out by the EKF until the end of the service life of the panel.

The PH, $\alpha - \lambda$ accuracy, RA, CRA, and convergence of the 10 panels are reported in Table 6. For PH and $\alpha - \lambda$ accuracy, $\alpha = 0.1$, $\lambda = 0.5$ are used. A larger PH indicates a better performance, which allows earlier prediction for the end of service life with more reliability. RA equals to one minus the relative error between the true RUL and the predicted RUL at a specific cycle. CRA is the mean of RA values accumulated at every cycle from the first cycle of RUL prediction to the last cycle. Therefore, the closer RA and CRA to 1, the higher the prediction accuracy is. As for convergence, the smaller the value, the faster is the convergence. From Table 6, we see that for all the 10 panels, the proposed prognostics method gives a large PH, high value of RA and CRA, and a relatively small value of convergence compared to their service lives. Therefore, the proposed prognostics method performs satisfactorily.

For illustration purposes, we provide the plots of the PH and $\alpha - \lambda$ accuracy for Panels 1–4, as shown in Figures 11 and 12, respectively.

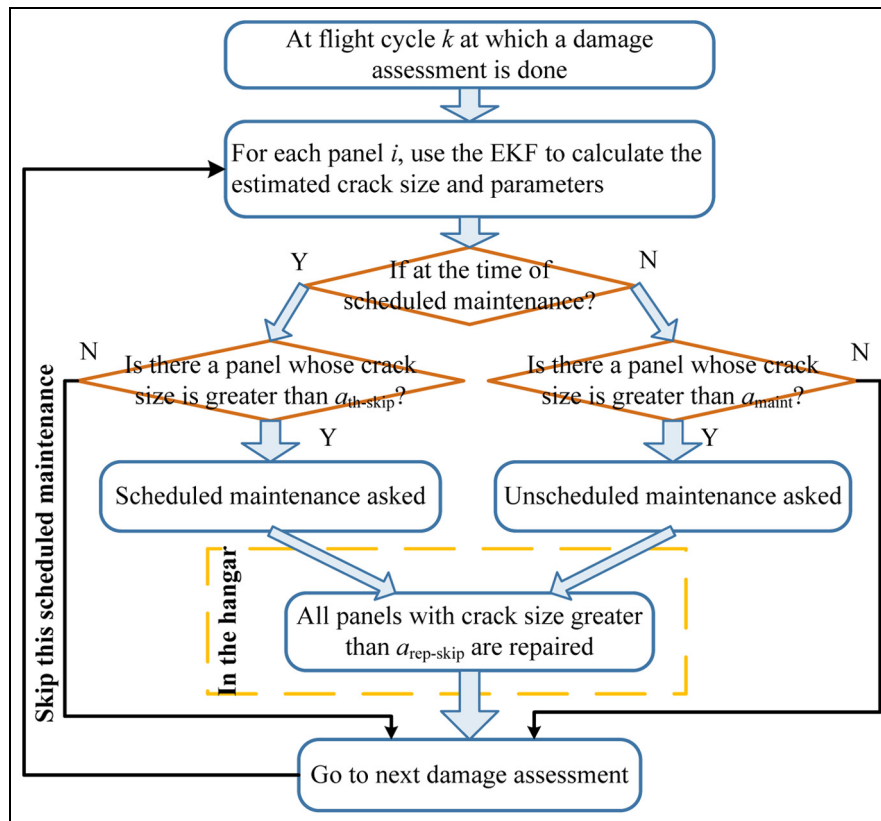


Figure 14. Flowchart of CBM-skip.

Appendix 4

Details of condition-based maintenance and condition-based maintenance-skip strategies

The structural health monitoring system is assumed to be used in condition-based maintenance (CBM) and CBM-skip, and damage assessment is done every 100 flights. In CBM, at each damage assessment, if the largest crack size in an aircraft exceeds a_{maint} , unscheduled maintenance is triggered immediately without considering the scheduled maintenance (Figure 5), that is, the maintenance could occur anytime unexpectedly, outside of the 10 scheduled maintenance stops. Once unscheduled maintenance is requested, all the panels with a crack size larger than a repair threshold $a_{\text{rep-CBM}}$ are repaired. Figure 13 illustrates a flowchart of CBM.

In contrast, CBM-skip takes into account the scheduled maintenance but aims at skipping some unnecessary early scheduled maintenance. The flowchart of CBM-skip is shown in Figure 14. At each scheduled maintenance stop, if there is no crack exceeding a threshold $a_{\text{th-skip}}$, then the current scheduled maintenance is skipped. Note that $a_{\text{th-skip}}$ can be much less conservative than the repair threshold of scheduled maintenance since damage assessment in CBM-skip is carried out very frequently outside of the scheduled maintenance stops. If there is a crack, which grows beyond a_{maint} between two consecutive scheduled maintenance stops, then an unscheduled maintenance is triggered at once and all panels with crack size greater than $a_{\text{rep-skip}}$ are repaired.